Journal of Luminescence 220 (2020) 116953

Contents lists available at ScienceDirect

Journal of Luminescence

journal homepage: http://www.elsevier.com/locate/jlumin

Interaction of proflavin with tryptophan in reverse micellar microenvironment of AOT: Photoinduced electron transfer probed by magnetic field effect

Banabithi Koley Seth [a,1,**], Abhishek Sau [a], Uttam Pal [b], Samita Basu [a], Brotati Chakraborty [c,*]

[a] Chemical Sciences Division, Saha Institute of Nuclear Physics, 1/AF Bidhannagar, Kolkata, 700064, India
[b] S.N. Bose National Centre for Basic Sciences, Kolkata, West Bengal, PIN- 700106, India
[c] Department of Chemistry, Bejoy Narayan Mahavidyalaya, Itachuna, Hooghly, West Bengal, PIN 712147, India

ARTICLE INFO

Keywords:
Laser flash photolysis
Magnetic field effect
Reverse micelle
Hyperfine interactions
$B_{1/2}$ value

ABSTRACT

Photoinduced electron transfer (PET) from a biological amine, tryptophan to a well-known acridine-derivative, proflavin has been investigated employing laser flash photolysis technique in heterogeneous AOT reverse micelles (RMs). In AOT RMs a significant magnetic field effect (MFF) on PET has been observed which authenticates the triplet spin states of the precursors of PET. The measurement of $B_{1/2}$ value gives an indication of the extent of hyperfine interactions present in the system in AOT medium. The cause of discrepancy between calculated and experimental $B_{1/2}$ values is explained. Further, it is observed that MFE decreases with increase in pool size of the RMs which highlights the importance of optimum separation between the corresponding radical ions pairs to maximize MFE.

1. Introduction

Electron transfer (ET) is one of the most fundamental reactions that occur in biological systems [1]. The study of the crucial role of ET in different proteins ranging from photosynthetic proteins to protein containing copper, iron-sulfur or heme group, becomes imperative day by day [2–7]. Generally in proteins, ET is a long distance phenomenon (>10 Å) which occurs through hopping between different protein residues in order to reduce the time that would be required for a single step tunneling from donor to acceptor [8–10]. Among the amino acid residues of proteins, Tryptophan (TrpH) in particular acts as a relay in such processes [11–16]. Among the four aromatic amino acids (i.e. phenylalanine, tyrosine, histidine, and tryptophan), TrpH is the only one which can donate and forms an ET-complex, as observed with riboflavin, serotonin (5-hydroxytryptamine), tryptamine derivatives, lysergic acid etc [17,18]. This kind of ET occurs from the π-electron pool of the indole system of residue to the acceptor [19]. TrpH also acts as a photo-triggered electron donor as observed in cryptochromes [20], DNA repairing by photolyase [21] etc. Further, when there is no electron acceptor nearby, TrpH undergoes ET with the backbone of the protein as observed in case of apo-myoglobin mutants, small cyclic peptides, and human γ–D-crystallin etc [22]. Recently, it has been observed that a "Tryprtophan triad" is able to make an ET channel during photoreduction of FAD in various protein families [23–26]. Therefore, the versatility of TrpH-mediated ET in proteins and its widespread occurrence in proteins, make TrpH a routine as well as pivotal probe in investigation of the dynamics of protein.

Proflavin (PF^+), an acridine derivative is well known for its antibacterial and antifungal properties against many gram-positive bacteria and is extensively used as an extrinsic probe to reveal biological intricacies as it is able to bind with DNA and proteins [27,28]. Further, its intrinsic fluorescence and triplet absorption properties make PF^+ an efficient probe for the investigations of ground and excited state phenomena [29]. It remains positively charged in a long range of pH (0.2–9.5) including biological pH [30]. Thus, it may act as a good electron acceptor which was confirmed by previous studies from our laboratory [31,32]. The interaction of PF^+ with aliphatic amine (e.g. triethylamine) [31] or aromatic amines (e.g. *N, N′*-dimethylaniline and 4,4′–bis (dimethylamino) diphenylmethane) [32] indicates the dependence of photoinduced electron transfer (PET) on the nature of acceptor

* Corresponding author.
** Corresponding author.
E-mail addresses: banabithi.koley-seth@durham.ac.uk (B. Koley Seth), brotati07@gmail.com (B. Chakraborty).
[1] Current address: Department of Chemistry, Durham University, Lower Mountjoy, South Road, Durham, DH1 3LE, United Kingdom.

https://doi.org/10.1016/j.jlumin.2019.116953
Received 11 October 2019; Received in revised form 30 November 2019; Accepted 5 December 2019
Available online 6 December 2019

molecules and the nature of the solvent matrices.

One of the most popular means of studying photoinduced processes like PET or excited-state intramolecular proton transfer is fluorescence spectroscopy [33–38]. In fact, the ultimate products and transient intermediates of PET reactions are usually estimated by steady-state and time-resolved absorption and fluorescence experiments respectively. However, since last few decades the application of an external magnetic field (MF) has been gaining importance along with the above mentioned experiments [39–48]. This is because the magnetic field effect (MFE) is quite competent to identify the initial spin state of the precursors of PET, one of the deciding factors for ultimate products, and to assess the intermediate distance in geminate spin-correlated radical pairs (RP)/radical ion pairs (RIP) produced as transients, which is very much useful to study 'distance-dependent' interactions in biomacromolecules.

The RPs/RIPs, which are formed in the due course of PET, are susceptible to be easily perturbed by external MF as they contain unpaired electrons. When the partners of the geminate RIPs undergo diffusion and are separated by an optimum distance where exchange interaction is negligible, the internal MF produced by electron-nuclear hyperfine interaction (HFI) can induce spin flipping, *i.e.* sufficient mixing of singlet (S) and triplet ($T_{\pm}$, T_0) states and promote intersystem crossing (ISC). In the absence of an external MF, leakage to the triplet surface is maximum. If an external MF of the order of HFI or higher is applied, then the degeneracy of the triplet spin states is removed and only $S \rightarrow T_0$ channel becomes operative. As a result, the population of the initial spin state of the RIPs formed during PET increases. If the initial spin state is singlet then there will be a predominance of recombination product while if it is triplet then more of free radicals will be formed.

We herein report the interaction study of positively charged PF^+ with TrpH, a biologically available electron donor system, in homogeneous medium (tris-NaCl/HCl buffer medium, at biological pH 7.4) as well as reverse micellar heterogeneous medium of sodium bis-(2-ethylhexyl) sulfosuccinate (aerosol OT or AOT) using laser flash photolysis (LFP) technique corroborated with an external MF. Choice of reverse micelle (RMs) is significant in this purpose as in RMs, the micellar interface and aqueous phase yield a unique and versatile reaction field for the study of biochemical processes [49]. Photogenerated ions produced through PET reactions prefer to recombine in homogeneous medium. Organized media can effectively prevent this subsequent recombination and control back ET by manipulating electrostatic and spatial effects. Amphiphilic molecules are capable of self-assembly and can thus associate to form spatially organized pockets. Charged amphiphiles are also capable of displaying a strong electric field in their vicinity. These hydrophobic and electrostatic interactions lead to efficient partitioning of the substrates. These systems are also used for probing local environment on the distance scale of angstroms. Moreover micelles, RMs and vesicles are model membrane mimetic systems. Therefore, understanding PET in these simple systems can help in our understanding of biological PET reactions. The confined systems prolong the lifetimes of the radicals or radical ion pairs formed as a consequence of PET reactions and also maintain the optimum distance between them so that the geminate characteristic, which is an important factor for obtaining appreciable MFE, is preserved. Further, biological nanocavities like protein structures may impart pseudo-confinement to the radical ions which may help in to maintain the optimum conditions required to observe substantial MFE [50–52]. In fact, we have previously reported the interaction of PF^+ with human serum albumin (HSA), a serum protein which houses a single tryptophan residue. Using LFP we found that PET occurs from the tryptophan residue to PF^+ and observation of MFE helped us to conclude that the parent spin state of the precursor of PET is triplet [52]. MFE is observed prominently when the partner radical/radical ions are separated by 10–20 Å. In case of PF^+-HSA system, the stereoview of the docked conformation showed that the distance between the tryptophan residue and PF^+ is 12.93 Å, which explained the observed MFE. The complex structure of the protein imparts pseudo-confinement to the radical ions, which consequently leads to appreciable MFE. The present communication is a quest to explore that whether PET takes place between PF^+ and tryptophan in another confined system of AOT, which itself is a unique solvent matrix.

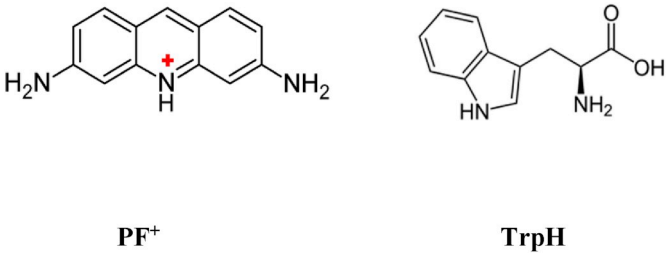

PF^+ **TrpH**

Scheme 1. Chemical structures of PF^+ and TrpH.

2. Experimental

2.1. Instrumentation

LFP technique was used to detect the non-fluorescent transients formed during PET reactions. The transient absorption spectra were measured by using a nanosecond flash photolysis setup (Applied Photophysics) having a Q-switched, Neodymium doped Yttrium Aluminium Garnet (Nd:YAG) laser (Lab series, Model Lab 150, Spectra Physics, USA.) (described earlier) [53]. The fundamental emission at 1064 nm is generated from the active medium Nd^{3+} ($^4F_3 \rightarrow {}^4I_{11/2}$). Other harmonics can be produced by frequency conversion in the nonlinear potassium dideuterium phosphate (KD*P) crystals.

In our experiments, the sample was excited by 355 nm laser light with FWHM ≈8 ns. Absorption of light from a pulsed Xe lamp (150 W) at right angle to the laser beam was employed to detect the newly generated transient species in the system. The photomultiplier (R928) output was fed into an Agilent Infiniium oscilloscope (DSO8064A, 600 MHz, 4 Gs/s) and the data were transferred to a computer using IYONIX software. MFEs on the transient absorption spectra were explored by passing direct current through a pair of electromagnetic coils placed inside the sample chamber. The strength of MF was varied from 0.0 to 0.08 T. Before carrying out the experiments, all samples were deaerated properly by argon gas. During the experiments no degradation of the samples was observed. The software Origin 8.0 was used for the analyses of data.

2.2. Materials

Proflavin, L-tryptophan, tris buffer and AOT were procured from Sigma Aldrich and used without further purification. Structures of the chemicals used are shown in Scheme 1 pH of 0.01 M tris-HCl/NaCl buffer was maintained at biological pH 7.4. To get homogeneous solutions, PF^+ and TrpH were dissolved in tris buffer medium. The heterogeneous medium AOT/H_2O/n-heptane reverse micelle (AOT RMs) was prepared by dissolving measured amount of solid AOT in n-heptane by volumetric method. Subsequently triple distilled water was added to the solution to obtain appropriate value of w_0, where w_0 denotes the ratio of molar concentration of water to AOT. AOT RMs form a well characterized monodispersed spherical RMs in n-heptane and are able to solubilize a large quantity of water inside [54]. For a known concentration of AOT the size of the entrapped water pool depends on the w_0 value [55], where,

$$w_0 = [\text{polar solvent}] / [\text{surfactant}] \quad (1)$$

The diameter (d) of a RM depends on these w_0 values, which can be calculated (in nm) using the following equation [56],

$$d = 0.29 w_0 + 1.1 \quad (2)$$

Solutions were made by dissolving measured amount of solid AOT in n-heptane by volumetric method. Subsequently triple distilled water

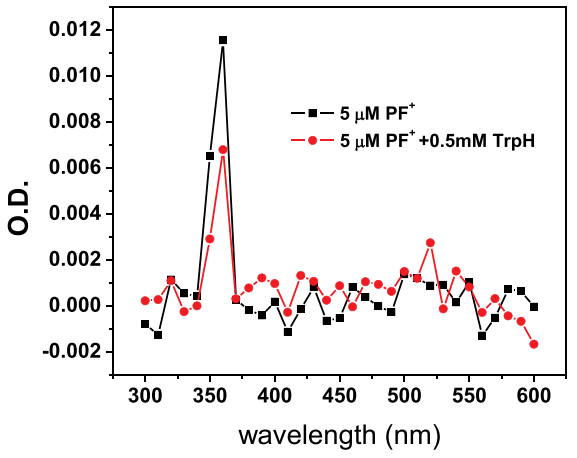

A

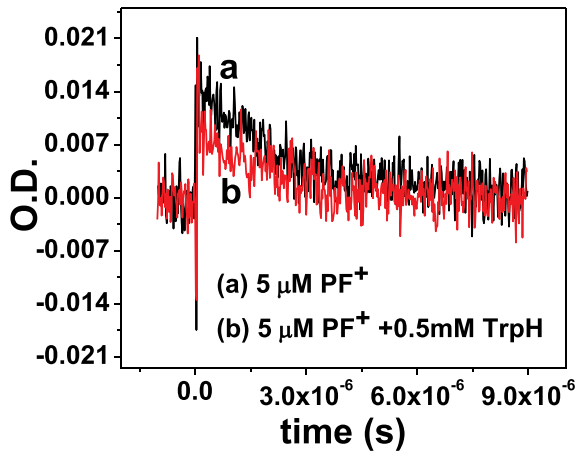

B

Fig. 1. A: Transient absorption spectra of (a) PF^+ (5 μM) and (b) PF^+ (5 μM) + TrpH (0.5 mM) in buffer medium of pH 7.4 at a delay of 0.5 μs after the laser pulse at 355 nm. B: Decay profiles of (a) PF^+ (5 μM) and (b) PF^+ (5 μM) + TrpH (0.5 mM) in buffer medium at 360 nm after the laser flash at 355 nm.

was added to the solution to obtain appropriate value of w_0, where w_0 denotes the ratio of molar concentration of water to AOT. The w_0 values were kept as 10, 15 and 20. The concentration of AOT in all RMs was maintained at 0.1 M. The mixtures were then thoroughly shaken and sonicated for 10 min to obtain a transparent and thermodynamically stable solution. The optimum concentration of water in AOT is determined using absorption spectra. As TrpH is not easily soluble in AOT, therefore it was at first dissolved in very small amount of tris buffer (<2.5%) followed by the water adjustment to maintain w_0 in AOT. All the measurements were performed at room temperature.

2.3. Theoretical modeling

Proflavin radical structure (with 111 electrons) was geometry optimized and the Fermi Contact coupling constants were computed using unrestricted B3LYP [57,58] functional with EPR-III basis set, which is optimized for the computation of hyperfine coupling constants by Density Functional Theory methods, specifically B3LYP [59]. EPR-III is a triple-zeta basis set which includes diffuse functions, double d-polarizations and a single set of f-polarization functions (as depicted in Fig. S1). Further, the s-part is improved to better describe the nuclear regions. Fig. S2 shows labeled structure of proflavin used for theoretical modeling.

Classical molecular dynamics (MD) simulation was performed on proflavin and Trp in water following previously published protocol [60]. Coulombic and van der Waals interaction energies between proflavin and Trp was computed over the 4.8 ns of simulation time. A few probable complexes having pi-stacking, hydrogen bonding or pi-cation interactions were further optimized using density functional theory (DFT) following previously published protocol using B3LYP exchange correlation functional and 6–31 g+(d) basis set [61]. Grimme's empirical dispersion correction (GD3) was added to account for the non-bonded intermolecular interactions [62]. All the optimization were done in polarizable continuum model (IEFPCM) of water, where the molecule was placed in a solvation cavity and a constant dielectric field was assumed on the outside [63]. UV visible spectra of the complex formed between proflavin and TrpH was computed using time dependent density functional theory (TD-DFT) with same exchange correlations and basis sets, which was used for geometry optimization [64]. Fig. S3 shows the optimized geometry of the most favourable complex formed

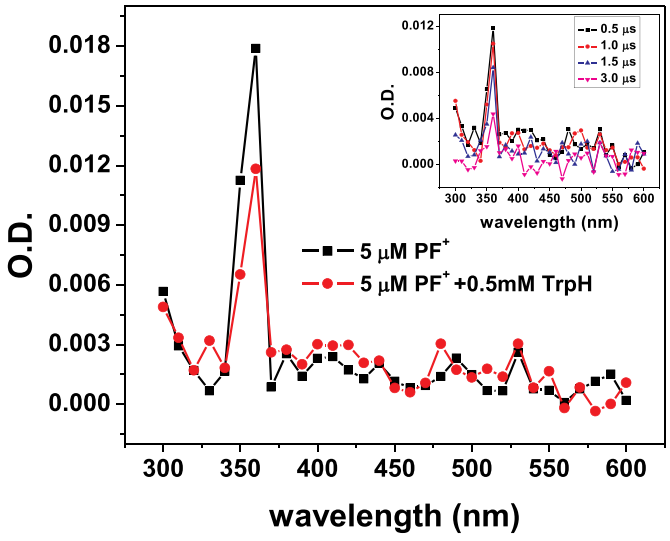

A

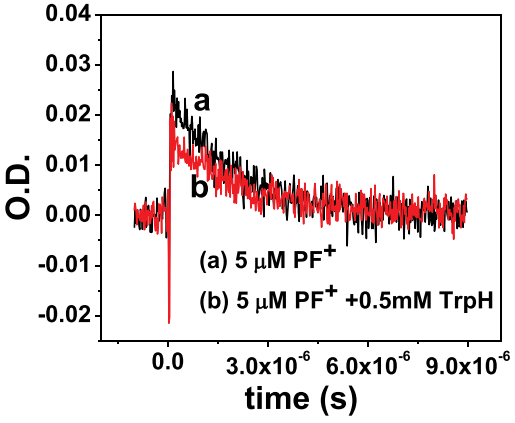

B

Fig. 2. A: Transient absorption spectra of (a) PF^+ (5 μM) and (b) PF^+ (5 μM) + TrpH (0.5 mM) in AOT RM medium of $w_0 = 10$ at a delay of 0.5 μs after the laser pulse at 355 nm. Inset shows time-resolved transient absorption spectra of PF^+ (5 μM) + TrpH (0.5 mM) at 0.5 μs (■), 1.0 μs (●), 1.5 μs (▲) and 3.0 μs (▼) after the laser pulse at 355 nm in AOT RMs of $w_0 = 10$. B: Decay profiles of (a) PF^+ (5 μM) and (b) PF^+ (5 μM) + TrpH (0.5 mM) in AOT RM medium of $w_0 = 10$ at 360 nm after the laser flash at 355 nm.

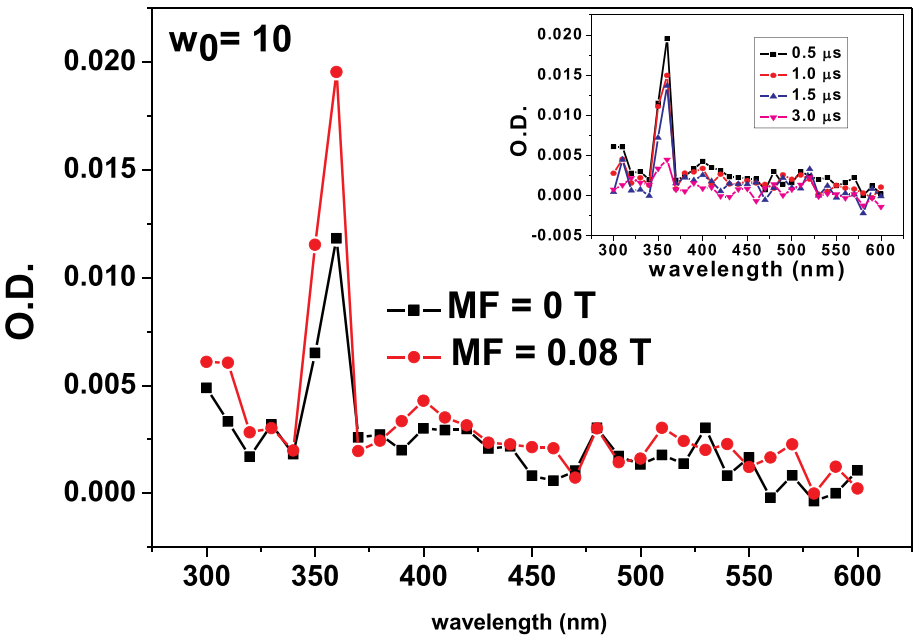

A

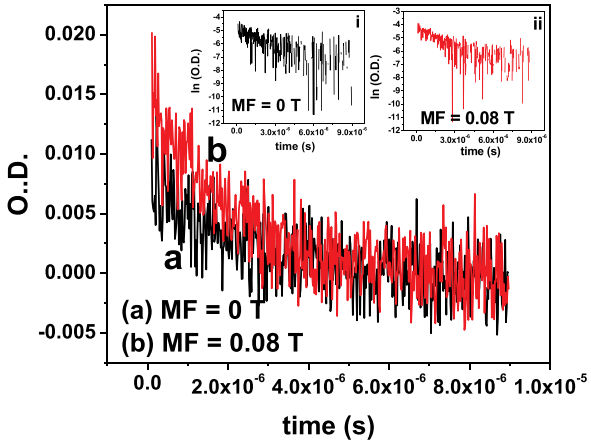

B

Fig. 3. A: Transient absorption spectra of PF^+ (5 μM) + TrpH (0.5 mM) in absence and presence of MF at a delay of 0.5 μs after the laser pulse at 355 nm in AOT RMs of w_o = 10. Inset shows time-resolved transient absorption spectra of PF^+ (5 μM) + TrpH (0.5 mM) in presence of MF at 0.5 μs (■), 1.0 μs (●), 1.5 μs (▲) and 3.0 μs (▼) after the laser pulse at 355 nm in AOT RMs of w_o = 10. B: Decay profiles of PF^+ (5 μM) + TrpH (0.5 mM) in AOT RMs of w_o = 10 at 360 nm in absence and presence of external MF. Insets (i) & (ii) depict logarithmic representations of decay profiles of PF^+ (5 μM) + TrpH (0.5 mM) in AOT RMs of w_o = 10 at 360 nm in absence and presence of external MF respectively.

between proflavin and TrpH.

3. Results and discussion

3.1. LFP in conjunction MF

3.1.1. Homogeneous medium

In tris-HCl/NaCl buffer medium (pH = 7.4), the triplet state peak of PF^+ is observed at 360 nm. On addition of TrpH to a solution of PF^+, there is appreciable quenching of absorbance of $^3PF^+$ at 360 nm accompanied by formation of a small new hump at 400 nm as shown in Fig. 1A. Further, there is also small increase in absorbance at 520 and 560 nm. As suggested in literature reports, emergence of a distinctly new hump at 400 nm is attributed to the formation of PF• [31,32,52]. Previous reports suggest that the transient absorption spectral signatures of $TrpH^{\bullet+}$ are found at 350 nm as well as 560 nm and that of Trp• is at 510 nm [52]. Decay profiles of 5 μM solution of PF^+ in buffer medium in absence and presence of TrpH at 360 nm after the laser flash are depicted in Fig. 1B.

3.1.2. Heterogeneous medium

The number of water molecules per AOT is usually defined by w_0 parameter (as represented in equation (2)). The interior of RMs is highly heterogeneous in nature [54,55], consisting of two types of aqueous environments, i.e. interfacial water (or bound water) and core water (free water). The interfacial water molecules resemble the water molecules at the immediate vicinity of the bioaggregates such as proteins, membranes and mitochondria [65,66], while core water shows bulk-water like properties. Thus, AOT RMs serve as excellent biomimics for exploration of biologically confined water molecules [67,68]. Solvation time and relaxation of a highly structured nanopool of water are found to be slower by several orders of magnitude compared to those of ordinary water [65]. The inhomogeneous dynamics of water inside the nanopool is because of its differential H-bonding behaviour in two different regions of RMs [67–72]. Some workers have rationalized this differential behavior of water by considering the interactions among

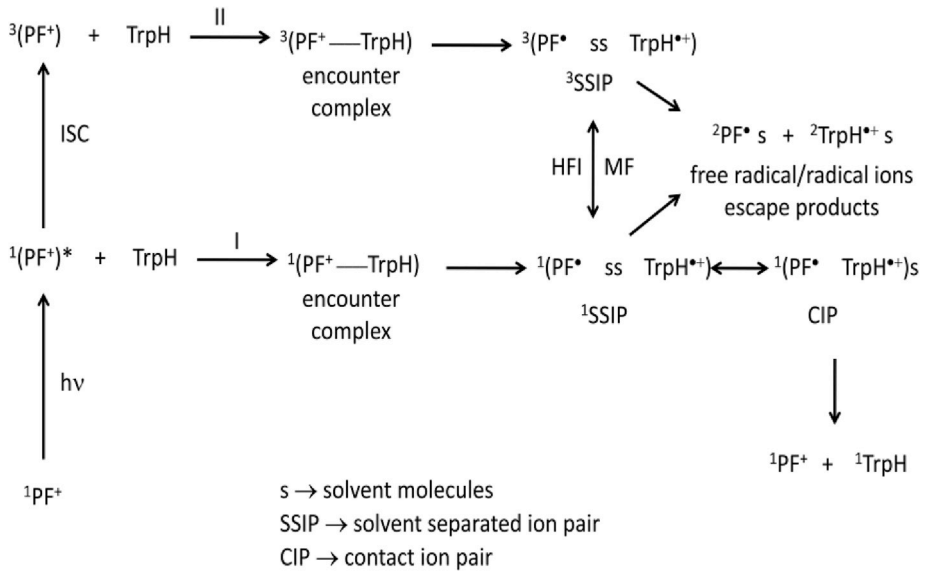

Scheme 2. Proposed reaction pathways.

water molecules and surfactant head groups, while other believe that the nature of confinement is responsible for such a behaviour [73,74].

In AOT RMs medium of $w_0 = 10$, the triplet state peak of PF^+ is observed at 360 nm similar to that in homogeneous medium. Upon addition of TrpH, there is quenching of the spectral signature of PF^+ along with the formation of a new hump at 400 nm and also a slight increase in absorbance at 520 nm as well as at 550 nm as shown in Fig. 2A. These observations are very similar to those obtained in homogeneous medium and probably suggest that PET takes from TrpH to PF^+ which leads to the formation of $PF^•$ and $TrpH^{•+}$. Inset of Fig. 2A shows time-resolved transient absorption spectra of PF^+ (5 μM) + TrpH (0.5 mM) at 0.5, 1.0, 1.5 and 3.0 μs after triggering of the laser pulse in AOT RMs of $w_0 = 10$. Decay profiles of 5 μM solution of PF^+ in AOT RM medium of $w_0 = 10$ in absence and presence of TrpH at 360 nm after the laser flash are depicted in Fig. 2B.

Now the pertinent question is why the signature of $Trp^•$ is observed as evident from increase in absorbance in presence of TrpH around 500 nm as depicted in Fig. 2A? Earlier reports suggest that electron transfer followed by proton transfer involving the TrpH residue of protein is a common phenomenon [75] and has also been observed previously by our group while studying the interaction of PF^+ with HSA [52]. Thus, it may be proposed that PET takes place from TrpH to PF^+. As PF^+ bears a unipositive charge at pH 7.4, PF^+ yields a radical ($PF^•$) instead of a radical anion ($PF^{•-}$) in the due course of PET [52], which eventually produces the spin-correlated geminate pair ($TrpH^{•+}$ $PF^•$) that undergoes proton transfer within the geminate cage to yield spin-correlated ($Trp^•$ $PFH^{•+}$). The proton transfer step may be represented as follow:

$$PF^• + TrpH^{•+} \rightarrow PFH^{•+} + Trp^• \quad (3)$$

The transient absorption spectra of PF^+ (5 μM) + TrpH (0.5 mM) in absence and presence of a weak external MF of 0.08 T in AOT RMs medium of $w_0 = 10$ are shown in Fig. 3A. Inset of Fig. 3A shows time-resolved transient absorption spectra of PF^+ (5 μM) + TrpH (0.5 mM) in presence of MF at 0.5, 1.0, 1.5 and 3.0 μs after triggering of the laser pulse in AOT RMs of $w_0 = 10$. In presence of MF, there is augmentation of absorbance at 360, 400, 510 and 560 nm. The most appreciable MFE is observed in the region of 350–360 nm which is the spectral signature of $TrpH^{•+}$. The decay profiles of the transient at 360 nm (as depicted in Fig. 3B) show an increase in lifetime from 1.77 μs (in absence of MF) to 2.45 μs (in presence of MF). This implies that the precursors of PET are triplet-born. In absence of MF, increase in absorbance at 360 nm on addition of TrpH to PF^+ solution is not clearly understood because $^3PF^+$

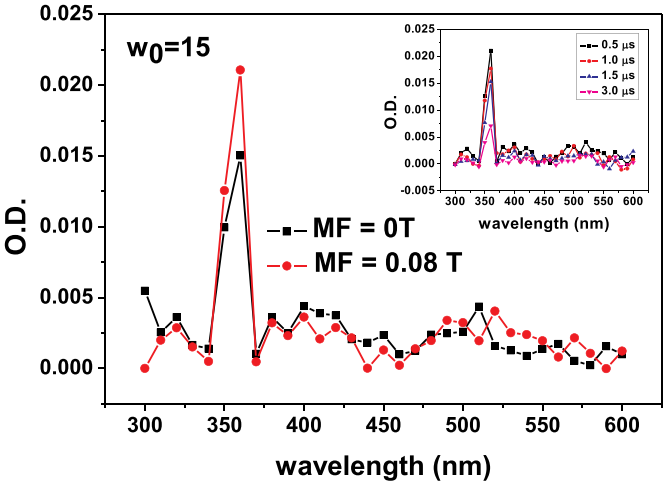

Fig. 4. Transient absorption spectra of PF^+ (5 μM) + TrpH (0.5 mM) in absence and presence of MF at a delay of 0.5 μs after the laser pulse at 355 nm in AOT RMs of $w_0 = 15$. Inset shows time-resolved transient absorption spectra of PF^+ (5 μM) + TrpH (0.5 mM) in presence of MF at 0.5 μs (■), 1.0 μs (●), 1.5 μs (▲) and 3.0 μs (▼) after the laser pulse at 355 nm in AOT RMs of $w_0 = 15$.

has characteristic peak at 360 nm and shows an overall quenching as evident from Fig. 2A. It is only the use of MF which helps to reveal that a radical ion $TrpH^{•+}$ is formed at 360 nm. Insets (i) and (ii) of Fig. 3B are the logarithmic representations of decay profiles of Fig. 3B to check their monoexponential nature. Previous study suggests that the signature of $PFH^{•+}$ is at 550 nm while that of $TrpH^{•+}$ is at 560 nm [46]. Therefore, increase in absorbance at 550 nm may imply the increase in yields of both $PFH^{•+}$ and $TrpH^{•+}$. Thus, the observed MFE may arise due to both the types of spin correlated geminate pairs, *viz*, ($TrpH^{•+}$ $PF^•$) as well as ($Trp^•$ $PFH^{•+}$). Moreover, MFE at 360 and 400 nm confirms that the initial spin state of the precursors of PET is triplet and pathway II in Scheme 2 is preferred over pathway I. The proposed mechanism of reaction is depicted in Scheme 2 although the proton transfer step is not shown in this Scheme.

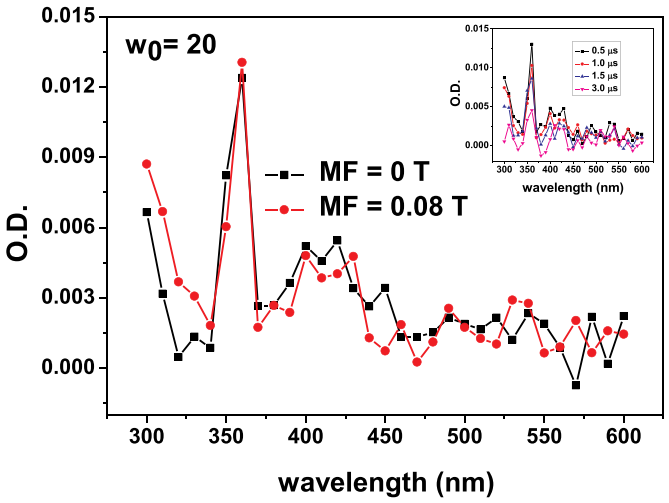

Fig. 5. Transient absorption spectra of PF^+ (5 μM) + TrpH (0.5 mM) in absence and presence of MF at a delay of 0.5 μs after the laser pulse at 355 nm in AOT RMs of $w_0 = 20$. Inset shows time-resolved transient absorption spectra of PF^+ (5 μM) + TrpH (0.5 mM) in presence of MF at 0.5 μs (■), 1.0 μs (•), 1.5 μs (▲) and 3.0 μs (▼) after the laser pulse at 355 nm in AOT RMs of $w_0 = 20$.

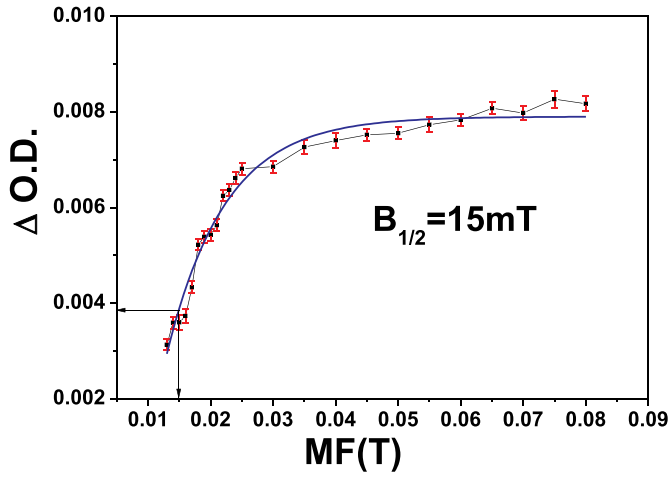

Fig. 6. Variation of ΔOD with external MF for PF^+ (5 μM) + TrpH (0.5 mM) system at 510 nm in AOT RMs of $w_0 = 10$ at 0.5 μs delay of laser pulse at 355 nm.

Table 1
Decay rate constant (k) and relative radical escape yield (γ) of $TrpH^{\bullet+}$ in absence and presence of MF. [^{a} Arbitarily taken]. γ = Absorbance (MF, x μs) /Absorbance (MF = 0, x μs).

Wavelength (nm)	w_0	MF (T)	Decay rate constant k (s^{-1})	γ
360	10	0	5.6×10^5	1.00[a]
		0.08	4.0×10^5	1.72
	15	0	5.3×10^5	1.00[a]
		0.08	4.9×10^5	1.40
	20	0	4.9×10^5	1.00[a]
		0.08	4.4×10^5	1.08

$$^1(TrpH^{\bullet+}\ PF^{\bullet}) \xleftrightarrow[MF]{HFI} {}^3(TrpH^{\bullet+}\ PF^{\bullet}) \quad (4)$$

and

$$^1(Trp^{\bullet}\ PFH^{\bullet+}) \xleftrightarrow[MF]{HFI} {}^3(Trp^{\bullet}\ PFH^{\bullet+}) \quad (5)$$

Further, Figs. 4 and 5 depict the effect of MF on transient absorption spectra of PF^+ (5 μM) + TrpH (0.5 mM) in varying water pool size of RMs. Also, insets of Figs. 4 and 5 show time-resolved transient absorption spectra of PF^+ (5 μM) + TrpH (0.5 mM) in presence of MF at 0.5, 1.0, 1.5 and 3.0 μs after triggering of the laser pulse in AOT RMs of $w_0 =$ 15 and 20 respectively. It is observed that MFE varies with w_0 and as the water pool size of the RMs is increased, the extent of MFE becomes less prominent. A direct estimation of variation of MFE with w_0 can be obtained from the values of escape yield as depicted in Table 1. Decay profiles of PF^+ (5 μM) + TrpH (0.5 mM) in absence and presence of MF in AOT RMs of $w_0 = 15$ and 20 at 360 nm are depicted in Supporting Information (Figs. S4–S7). It is evident from Table 1 that on application of an external MF, decay rate decreases and correspondingly escape yield increases for each value of w_0 of RMs, which further supports the fact that the RIPs are generated in the triplet state. On application of MF, the conversion of the triplet RIP to the singlet RIP is hindered, and, as a result, the decay rates become slower, and escape yield is enhanced. Further, with increase in the values of w_0, the value of escape yield is found to decrease, which indicates that MFE is most prominent for $w_0 =$ 10 and gradually decreases with increase in water pool size of the RMs. Actually in RMs where $w_0 > 10$, water exhibits more of bulk water property and a floppy encounter complex is formed owing to free diffusion of water molecules [76], which consequently destabilizes the geminate SSIP because of loss in spin-correlation between RPs/RIPs. It is pertinent to mention here that the value of γ at 350 nm for PF^+-HSA system is 1.63 [52] which lies between the value of γ at 360 for $w_0 = 10$ and 15 in the present case.

It is well-known that the nature of confined water inside RMs is not similar like bulk water. However, with the increase in size of the water pool the nature of confined water becomes closer to that of bulk water although some researchers suggest that even in RMs with $w_0 = 40$, the number of confined water is too small to behave like bulk water [77]. It has also been reported that the dielectric relaxation is quite slower for confined water compared to bulk water [77]. With increase in water pool size of RMs the dielectric relaxation rate increases. Furthermore, in AOT RMs the 'acidity', i.e. free proton concentration is greater at interface compared to inside due to the anionic nature of the RMs. The availability of H^+ is less in RMs with smaller pool size due to the lesser number of water molecules compared to that with bigger pool size [78].

It is known that the tryptophan assigns its location in RMs at interface [79,80], whereas PF^+ remains in bulk water. As interfacial region of AOT is more acidic compared to bulk, this will help in formation of $TrpH^{\bullet+}$and not $Trp^{\bullet}$ as suggested by Burdi et. al., In 1997, Burdi and co-workers suggested that at low pH formation of $TrpH^{\bullet+}$is favoured over $Trp^{\bullet}$ [81]. In the present case, $TrpH^{\bullet+}$which is formed due to electron transfer, will try to come out of the interfacial region and approach free water where it can get stabilized by solvation; whereas $PF^{\bullet}$ will try to approach the interface. Again $PF^{\bullet}$ will have a tendency to abstract H^+ from $TrpH^{\bullet+}$or from the bound water at interface which leads to formation of $PFH^{\bullet+}$and $Trp^{\bullet}$.

The comparison between the spectra of PF^+ in absence and presence of TrpH clearly signifies the presence of $TrpH^{\bullet+}$. Owing to the occurrence of secondary processes the signature of $PF^{\bullet}$, $PFH^{\bullet+}$ and $Trp^{\bullet}$ becomes somewhat insignificant. However, only in presence of MF the presence of the secondary species can be detected and it is significant in AOT RMs with water pool size $w_0 = 10$. It is pertinent to mention here that previous report suggests that AOT with water pool size around $w_0 =$ 7.5 gives the most stable structure due to the appropriate combination of attractive and repulsive electrostatic interactions, which also controls the spin and diffusion dynamics of RIPs to show MFE [82].

With increase in water pool size the formation of $TrpH^{\bullet+}$ as well as $PF^{\bullet}$ becomes prominent because of the increase of stability of $TrpH^{\bullet+}$ in

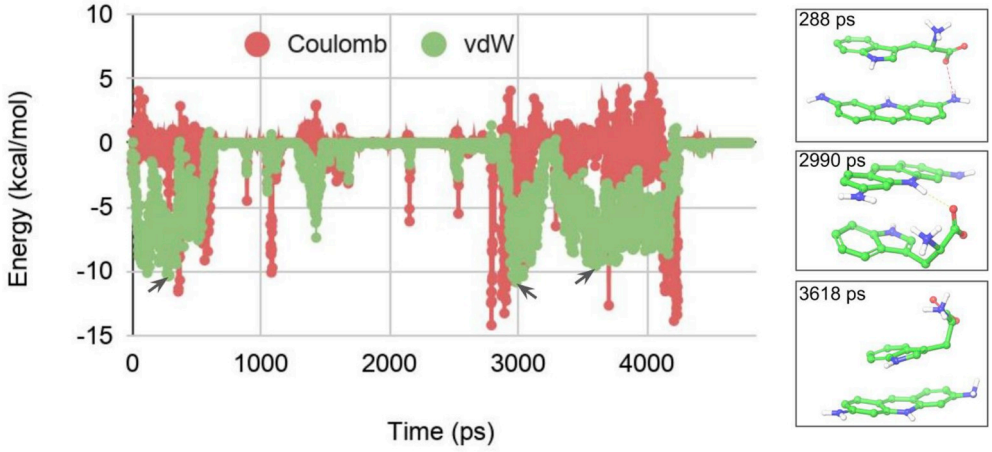

Fig. 7. Coulombic and van der Waals interaction energies of proflavin and Trp in water. Stacking interactions at three different times are shown on the right. Pi-cation and hydrogen bonding interactions between proflavin and Trp are marked with dotted lines. proflavin and Trp are shown in ball-and-stick model with C, N and O in green, blue and red, respectively. Only polar hydrogens are shown in white.

bulk water, since it faces much more repulsion from the acidic H^+ at the interface, whose concentration increases with increase in water pool size [77,78]. In fact, if the spectra of PF^+ in presence of TrpH in AOT RMs of $w_0 = 10$, 15 and 20 are compared (Figs. 3A, 4 and 5) it is found that in absence of MF, signature of presence of $PF^{\bullet}$ at 400 nm is prominent and its yield increases with increase in value of w_0. The lifetime at 400 nm for the aforementioned sample solution is almost insignificant in $w_0 = 10$, 1.43 μs in $w_0 = 15$ and 1.54 μs in $w_0 = 20$. However, as $TrpH^{\bullet+}$ remains inside water pool and $PF^{\bullet}$ tends to move towards the interface, lack of optimum separation distance between $TrpH^{\bullet+}$ and $PF^{\bullet}$ leads to low MFE at higher w_0 owing to loss of spin correlation.

The extent of HFI present in the system has been determined by measuring the $B_{1/2}$ value, the MF corresponding to the half saturation of MFE. The value of $B_{1/2}$, has been determined experimentally from the changes in absorbance of transients with variation of externally applied MF as shown in Fig. 6. $B_{1/2}$ has also been calculated by following theoretical expressions [Eqs. (6) and (7)] established by Weller using quantitative co-relation between $B_{1/2}$ and HFI energy of the individual radical pair [83],

$$B_{1/2} = \frac{\left[2\left(B_1^2 + B_2^2\right)\right]}{B_1 + B_2} \tag{6}$$

where, B_i represents the effective nuclear MF at the unpaired electron in each radical. Further, those individual B_i values can also be determined following the equation [Eq. (7)] on the basis of the interaction study between nuclear spin (I_N) and the unpaired electron spin in each radical.

$$B_i = \left(\sum \alpha_{iN}^2 I_N (I_N + 1)\right)^{1/2} \tag{7}$$

The values of α_{iN} for $TrpH^{+\bullet}$ molecule in aqueous medium have been obtained from the literature [84]. On the other hand, the α_{iN} values of $PF^{\bullet}$ have been computed (Table S1, Figs. S1 and S2). The isotropic hyperfine coupling constants have been calculated from the Fermi-contact interactions (Table S2) i.e. the contact interaction occurs only for s-electrons since s-orbitals have non-zero electron density at the nucleus. The calculated $B_{1/2}$ values have been observed as 4.3 mT using B_i values for $TrpH^{+\bullet}$ and $PF^{\bullet}$ as 2.56 mT and 0.99 mT respectively. The experimental $B_{1/2}$ value is found to be 15 mT as depicted in Fig. 6.

The discrepancy between calculated and experimental $B_{1/2}$ values have already been observed with different geminate radical ion pair systems in homogeneous as well as heterogeneous media at high donor concentrations [45,85]. Several interpretations have been proposed like uncertainty broadening of energy levels due to hopping of electron between ionic and neutral donors in the near vicinity [86–88] or lifetime time shortening of the radical ion pairs due to quenching of excess donor [89], which leads to the broadening of the energy levels. Hence higher MF is required to overcome the hyperfine interactions and decouple the $T_{\pm}$ spin levels from T_0 and S. In the present case, the concentration of TrpH is much higher than that of PF^+ and both are confined in the heterogeneous reverse micellar medium. Considering the above mechanisms the discrepancy between calculated and experimental $B_{1/2}$ values could be well interpreted.

Higher experimental $B_{1/2}$ values due to saturation at very high fields were explained by Sakaguchi et al. and Ulrich et al. [90,91] by the role of diffusion which can limit the rate constant of recombination of geminate radical ions and the spin relaxation which needs higher field. For relaxation mechanism between $T_{\pm}$ and T_0 states, the ISC rate is controlled by anisotropic hyperfine interaction and Zeeman interaction within microsecond time scale and the rate increases with the increase in the field. However, the relaxation mechanism is operative in the field range of 0.05 T–2.0 T. Therefore, since in the present system the saturation of MFE reaches at a very low field, the role of relaxation mechanism becomes insignificant. Moreover, the proton abstraction by $PF^{\bullet}$ from $TrpH^{+\bullet}$ reduces the lifetime of the original geminate radical pair.

The Weller's formula for calculation of $B_{1/2}$ is applicable only when significant spin interactions are the isotropic hyperfine interaction between the electron and nuclear spins in each radical and the isotropic Zeeman interaction of the two electron spins with the applied MF [92]. In the present case, since the geminate radical ion pair lifetime increases as well as the concentration of one of the components is quite high the probability of reencounter or exchange within this confined medium cannot be over ruled. There may be an exchange zone where spin evolution is restricted. Moreover, in restricted environment there is possibility of spin-state mixing which is the interplay between HFI and fast dephasing process. The dephasing processes are induced by the fluctuation of inter-electron-spin-interactions, *i.e.* exchange interaction and/or dipole-dipole interaction caused by the diffusive motion of the radical pair in the confined medium [93].

3.2. MD simulation

Classical MD simulation shows that proflavin and Trp can interact in the ground state. Possible interactions include pi-stacking, pi-cation interaction and hydrogen bonding (Fig. 7). The complete trajectory of the simulation is shown in Video S1. In a confined environment of AOT reverse micelle, these interactions would be more stable facilitating PET. DFT study is performed on the favourable complexes observed in MD simulation to probe the charge transfer process. Analyses of the frontier

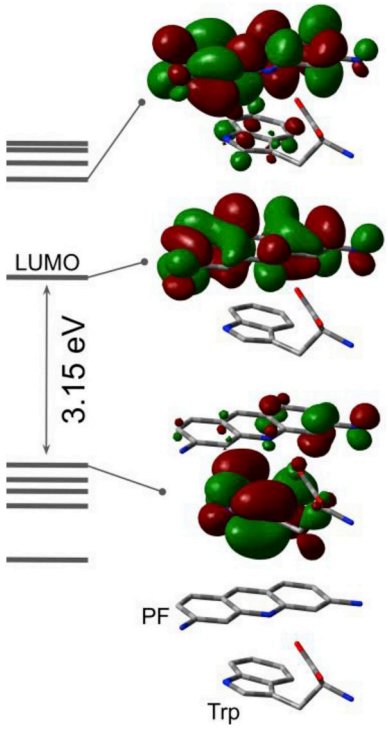

Fig. 8. Frontier molecular orbitals of the PF^{+}-Trp complex. Ladder on the left side represents relative energies.

molecular orbitals (Fig. 8) suggest that PET is possible from Trp to proflavin supporting the experimental results. TD-DFT calculations showed that the major electronic transitions occur from HOMO to LUMO+1 and {HOMO-1, HOMO-2, HOMO-3} to LUMO, which indicates electron transfer from Trp to proflavin. Band gap energies closely correspond to the wavelengths of the excitation light. Coordinate of the optimized geometry of the most favourable complex formed between proflavin and Trp is given in the supporting information (Table S3).

Supplementary data related to this article can be found at https://doi.org/10.1016/j.jlumin.2019.116953.

4. Conclusion

This paper reflects PET from a versatile biological amine TrpH to a routine probe used to reveal biological intricacies, PF^{+}. In the present case, PET occurs through radical pair mechanism in triplet state as revealed by MFE. The confined structure of AOT RMs helps to maintain the optimum separation distance between the RPs which results in observation of a prominent MFE. However, MFE decreases with increase in pool size of the RMs as the spin-correlation between the geminate RPs/RIPs formed during PET is lost due to increased separation distance induced by faster water dynamics in larger RMs. Further, the use of external MF authenticates the signature of $TrpH^{+\bullet}$ at 360 nm and confirms that the precursors of PET are triplet born. Had there been no MFE, the formation of $TrpH^{+\bullet}$ would probably go unnoticed. Finally, the probable cause of discrepancy between calculated and observed $B_{1/2}$ values has been discussed.

Declaration of competing interest

The authors declare no conflict of interest.

CRediT authorship contribution statement

Banabithi Koley Seth: Conceptualization, Methodology, Data curation, Writing - original draft. **Abhishek Sau:** Data curation. **Uttam Pal:** Software. **Samita Basu:** Conceptualization, Funding acquisition, Writing - review & editing. **Brotati Chakraborty:** Writing - original draft, Writing - review & editing.

Acknowledgement

The financial support from the project Biomolecular Assembly, Recognition and Dynamics (BARD) 12-R&D–SIN–5.04-0103 project of Department of Atomic Energy, Government of India is greatly acknowledged. Authors would like to thank Mrs. Chitra Raha for her kind assistance and technical support. A.S acknowledges UGC; Govt. of India [F2-32/1998 (SA-1)] for financial support.

Appendix A. Supplementary data

Supplementary data to this article can be found online at https://doi.org/10.1016/j.jlumin.2019.116953.

References

[1] R.A. Marcus, N. Sutin, Biochim. Biophys. Acta 811 (1985) 265.
[2] J.D. Rochaix, Biochim. Biophys. Acta 1807 (2011) 375.
[3] D.C. Johnson, D.R. Dean, A.D. Smith, M.K. Johnson, Annu. Rev. Biochem. 74 (2005) 247.
[4] O. Farver, I. Pecht, Coord. Chem. Rev. 255 (2011) 757.
[5] G.A. Mines, T. Pascher, S.C. Lee, J.R. Winkler, H.B. Gray, Chem. Biol. 3 (1996) 491.
[6] S.A. Schichman, T.E. Meyer, H.B. Gray, Inorg. Chim. Acta 243 (1996) 25.
[7] A. Robert, F. Benoit-Vical, B. Meunier, Coord. Chem. Rev. 249 (2005) 1927.
[8] H.B. Gray, B.G. Malmström, Biochemistry 28 (1989) 7499.
[9] C. Shih, A.K. Museth, M. Abrahamsson, A.M. Blanco-Rodriguez, A.J. Di Bilio, J. Sudhamsu, B.R. Crane, K.L. Ronayne, M. Towrie, A. Vicek Jr., J.H. Richards, J. R. Winkler, H.B. Gray, Science 320 (2008) 1760.
[10] H.B. Gray, J.R. Winkler, Proc. Natl. Acad. Sci. U.S.A. 102 (2005) 3534.
[11] C. Aubert, M.H. Vos, P. Mathis, A.P.M. Eker, K. Brettel, Nature 405 (2000) 586.
[12] W.H. Qiu, T.P. Li, L.Y. Zhang, Y. Yang, Y.T. Kao, L.J. Wang, D. Zhong, Chem. Phys. 350 (2008) 154.
[13] L.X.Q. Chen, J.W. Petrich, G.R. Fleming, A. Perico, Chem. Phys. Lett. 139 (1987) 55.
[14] J. Baldwin, C. Krebs, B.A. Ley, D.E. Edmondson, B.H. Huynh, J.M. Bollinger, J. Am. Chem. Soc. 122 (2000) 12195.
[15] J. Stubbe, W.A. van Der Donk, Chem. Rev. 98 (1998) 705.
[16] C. Consani, G. Auböck, F.V. Mourik, M. Chergui, Science 339 (2013) 1586.
[17] B. Pullman, A. Pullman, Proc. Natl. Acad. Sci. U. S. A. 44 (1958) 1197.
[18] I. Isenberg, A. Szent-Gyorgyi, Proc. Natl. Acad. Sci. U. S. A. 44 (1958) 857.
[19] I. Isenberg, A. Szent-györgyi, Proc. Natl. Acad. Sci. U. S. A. 45 (1959) 1229.
[20] D. Immeln, A. Weigel, T. Kottke, J.L. Pérez Lustres, J. Am. Chem. Soc. 134 (2012) 12536.
[21] M. Byrdin, V. Sartor, A.P.M. Eker, M.H. Vos, C. Aubert, K. Brettel, P. Mathis, Biochim. Biophys. Acta 1655 (2004) 64.
[22] R. Monni, A.A. Haddad, F.V. Mourik, G. Auböck, M. Chergui, Proc. Natl. Acad. Sci. U. S. A. 112 (2015) 5602.
[23] Y.M. Gindt, E. Vollenbroek, K. Westphal, H. Sackett, A. Sancar, G.T. Babcock, Biochemistry 38 (1999) 3857.
[24] C. Aubert, M.H. Vos, P. Mathis, A.P. Eker, K. Brettel, Nature 405 (2000) 586.
[25] J. Brazard, A. Usman, F. Lacombat, C. Ley, M.M. Martin, P. Plaza, L. Mony, M. Heijde, G. Zabulon, C. Bowler, J. Am. Chem. Soc. 132 (2010) 4935.
[26] T. Biskup, E. Schleicher, A. Okafuji, G. Link, K. Hitomi, E.D. Getzoff, E.D.S. Weber, Angew. Chem. Int. Ed. 48 (2009) 404.
[27] W.E. Lee, W.G. Galley, Biophys. J. 54 (1988) 627.
[28] B. Chakraborty, S. Basu, J. Lumin. 129 (2009) 34.
[29] -W.A. Noyes Jr., G.S. Hammond, G.N. Pitts Jr., In advances in photochemistry, in: Chapter - Phosphorescence and Delayed Fluorescence from Solutions, C. A. Parker, John Wiley & Sons, Inc. London, 1964.
[30] M.P. Pileni, M. Gratzel, J. Phys. Chem. 84 (1980) 2402.
[31] B. Chakraborty, S. Basu, Chem. Phys. Lett. 477 (2009) 382.
[32] B. Chakraborty, S. Basu, Chem. Phys. Lett. 487 (2010) 51.
[33] M. Kumbhakar, S. Nath, H. Pal, A.V. Sapre, T. Mukherjee, J. Chem. Phys. 119 (2003) 388.
[34] A. Chakraborty, D. Chakraborty, P. Hazra, D. Seth, N. Sarkar, Chem. Phys. Lett. 382 (2003) 508.
[35] Z. Lou, P. Li, K. Han, Acc. Chem. Res. 48 (2015) 1358.
[36] F. Yu, P. Li, G. Li, G. Zhao, T. Chu, K. Han, J. Am. Chem. Soc. 133 (2011) 11030.
[37] S.Y. Yin, S.S. Sun, M. Pan, L. Chen, Z. Wang, Y.J. Hou, Y.N. Fan, H.P. Wang, C. Y. Su, J. Photochem. Photobiol., A 355 (2018) 377.
[38] A.C. Sedgwick, X. Sun, G. Kim, J. Yoon, S.D. Bull, T.D. James, Chem. Commun. 52 (2016) 12350.
[39] U.E. Steiner, T. Ulrich, Chem. Rev. 89 (1989) 51.
[40] K. Bhattacharya, M. Chowdhury, Chem. Rev. 93 (1993) 507.
[41] C.B. Grissom, Chem. Rev. 95 (1995) 3.
[42] T. Sengupta, S.D. Choudhury, S. Basu, J. Am. Chem. Soc. 126 (2004) 10589.

[43] A. Bose, D. Dey, S. Basu, J. Phys. Chem. A 112 (2008) 4914.
[44] D. Dey, A. Bose, N.R. Pramanik, S. Basu, J. Phys. Chem. A 112 (2008) 3943.
[45] S. Dutta Choudhury, S. Basu, J. Phys. Chem. A 109 (2005) 8113.
[46] B. Chakraborty, S. Basu, Chem. Phys. Lett. 493 (2010) 76.
[47] B. Chakraborty, P. Mitra, S. Basu, RSC Adv. 5 (2015) 81533.
[48] B. Chakraborty, S. Basu, Appl. Magn. Reson. 42 (2012) 5.
[49] P.L. Luisi, M. Giomini, M.P. Pileni, B.H. Robinson, Biochim. Biophys. Acta 947 (1988) 209.
[50] T. Ulrich, U.E. Steiner, W. Schlenker, Tetrahedron 42 (1986) 6131.
[51] H. Yonemura, H. Nakamura, T. Matsuo, Chem. Phys. 162 (1992) 69.
[52] B. Chakraborty, A. Sinha Roy, S. Dasgupta, S. Basu, J. Phys. Chem. A 114 (2010) 13315.
[53] B. Koley Seth, A. Ray, A. Saha, P. Saha, S. Basu, J. Photochem. Photobiol. B Biol. 132 (2014) 72.
[54] N.E. Levinger, Science 298 (2002) 1722.
[55] M.K. Sarangi, S. Basu, Chem. Phys. Lett. 506 (2011) 205.
[56] T. Kinugasa, A. Kondo, S. Nishimura, Y. Miyauchi, Y. Nishii, K. Watanabe, H. Takeuchi, Colloids Surf., A 204 (2002) 193.
[57] C. Lee, W. Yang, R.G. Parr, Phys. Rev. B. 37 (1988) 785.
[58] A.D. Becke, J. Chem. Phys. 98 (1993) 5648.
[59] V. Barone, In recent advances in density functional methods, in: Of Recent Advances In Computational Chemistry, vol. 1, WORLD SCIENTIFIC, 1995, pp. 287–334. https://www.worldscientific.com/doi/abs/10.1142/9789812830586_0008.
[60] U. Pal, S.K. Pramanik, B. Bhattacharya, B. Banerji, N.C. Maiti, Springer Plus 5 (2016) 1121.
[61] A. Sau, K. Bera, U. Pal, A. Maity, P. Mondal, S. Basak, A. Mukherjee, B. Satpati, P. Sen, S. Basu, J. Phys. Chem. C 122 (2018) 23799.
[62] S. Grimme, J. Antony, S. Ehrlich, H. Krieg, J. Chem. Phys. 132 (2010) 154104.
[63] B. Mennucci, J. Tomasi, R. Cammi, J.R. Cheeseman, M.J. Frisch, F.J. Devlin, S. Gabriel, P.J. Stephens, J. Phys. Chem. A 106 (2002) 6102.
[64] D. Jacquemin, E.A. Perpète, X. Assfeld, G. Scalmani, M.J. Frisch, C. Adamo, Chem. Phys. Lett. 438 (2007) 208.
[65] K. Bhattacharyya, Chem. Commun. 28 (2008) 2848.
[66] S.K. Pal, A.H. Zewail, Chem. Rev. 104 (2004) 2099.
[67] K. Bhattacharyya, B. Bagchi, Chem. Rev. 100 (2000) 2013.
[68] K. Bhattacharyya, Acc. Chem. Res. 36 (2003) 95.
[69] A.K. Shaw, S.K. Pal, J. Phys. Chem. B 111 (2007) 4189.
[70] R. Biswas, N. Rohman, T. Pradhan, R. Buchner, J. Phys. Chem. B 112 (2008) 9379.
[71] H.S. Tan, I.R. Piletic, M.D. Fayer, J. Chem. Phys. 122 (2005) 175011.
[72] A.M. Dokter, S. Woutersen, H.J. Bakker, Proc. Natl. Acad. Sci. U.S.A. 103 (2006) 15355.
[73] M. Wong, J.K. Thomas, T. Nowak, J. Am. Chem. Soc. 99 (1977) 4730.
[74] D.E. Moilanen, N.E. Levinger, D.B. Spry, M.D. Fayer, J. Am. Chem. Soc. 129 (2007) 14311.
[75] D. Das, D.N. Nath, J. Phys. Chem. A 112 (2008) 11619.
[76] D.E. Moilanen, E.E. Fenn, D. Wong, M.D. Fayer, J. Phys. Chem. B 113 (2009) 8560.
[77] R.E. Riter, D.M. Willard, N.E. Levinger, J. Phys. Chem. B 102 (1998) 2705.
[78] P. Mukherjee, S. Gupta, S. Rafiq, R. Yadav, V.K. Jain, J. Raval, P. Sen, Langmuir 32 (2016) 1693.
[79] M.A.J. Rodgers, P.C. Lee, J. Phys. Chem. 88 (1984) 3480.
[80] S.M. Andrade, S.M.B. Costa, Photochem. Photobiol. 72 (2000) 444.
[81] D. Burdi, B.M. Aveline, P.D. Wood, J. Stubbe, R.W. Redmond, J. Am. Chem. Soc. 119 (1997) 6457.
[82] G. Eskici, P.H. Axelsen, J. Phys. Chem. B 120 (2016) 11337.
[83] A. Weller, H. Staerk, R. Treichel, Faraday Discuss. Chem. Soc. 78 (1984) 271.
[84] A.S. Kiryutin, O.B. Morozova, L.T. Kuhn, A.V. Yurkovskaya, P.J. Hore, J. Phys. Chem. B 111 (2007) 11221.
[85] H.W. Kruger, M.E. Michel-Beyerle, E.W. Knapp, Chem. Phys. 74 (1983) 205.
[86] E.W. Knapp, K. Schulten, J. Chem. Phys. 71 (1979) 1878.
[87] F. Nolting, H. Staerk, A. Weller, Chem. Phys. Lett. 88 (1982) 523.
[88] H. Staerk, W. Kûhnle, R. Treichel, A. Weller, Chem. Phys. Lett. 118 (1985) 19.
[89] D. Nath, M. Chowdhury, Chem. Phys. Lett. 109 (1984) 13.
[90] Y. Sakaguchi, H. Hayashi, Chem. Phys. Lett. 87 (1982) 539.
[91] T. Ulrich, U.E. Steiner, Chem. Phys. Lett. 112 (1984) 365.
[92] C.T. Rodgers, S.A. Norman, K.B. Henbest, C.R. Timmel, P.J. Hore, J. Am. Chem. Soc. 129 (2007) 6746.
[93] T. Miura, H. Murai, J. Phys. Chem. A 112 (2008) 2526.